7-15-2016

Polyisobutylene-paclitaxel conjugates with pendant carboxylic acids and polystyrene chains: Towards multifunctional stent coatings with slow drug release

John F. Trant
The University of Western Ontario

Mahmoud M. Abd Rabo Moustafa
The University of Western Ontario

Inderpreet Sran
The University of Western Ontario

Elizabeth R. Gillies
The University of Western Ontario

Polyisobutylene-Paclitaxel Conjugates with Pendant Carboxylic Acids and Polystyrene Chains: Towards Multifunctional Stent Coatings with Slow Drug Release

John F. Trant,[a†] Mahmoud M. Abd Rabo Moustafa[a†], Inderpreet Sran,[†] and Elizabeth R. Gillies[,*,†,§]

[†]Department of Chemistry, The University of Western Ontario, 1151 Richmond St., London, Canada, N6A 5B7`

[§]Department of Chemical and Biochemical Engineering, The University of Western Ontario, 1151 Richmond St., London, Canada, N6A 5B9

*Author to whom correspondence should be addressed; email: egillie@uwo.ca

Abstract

Drug-eluting stents are used in the treatment of atherosclerosis, where the incorporation of anti-proliferative or anti-inflammatory drugs decreases the rate of restenosis, the recurrence of artery narrowing. However, these stents can suffer from limitations such as drug depletion and delamination of the drug-eluting coating from the stent surface. Described here is an approach aimed at addressing these issues. Starting from a maleic anhydride adduct of polyisobutylene (PIB) prepared from butyl rubber, ring opening using paclitaxel (PTX) or a combination of PTX and polystyrene (PS) afforded covalent conjugates of PTX and PIB or PIB-PS graft copolymers

[a] JFT and MMARM contributed equally to this work.

bearing pendant carboxylic acids. When coated on stainless steel, the drug release was slower than that from a control coating that ressembles a clinical formulation comprising a physical mixture of a PS-PIB-PS triblock copolymer (SIBS) and PTX. The PTX conjugates also exhibited enhanced adhesion to stainless steel and increased tensile strength in comparison with the starting rubber. Cytotoxicity assays indicated that the materials did not leach toxic levels of PTX into cell culture media. Nevertheless, they were capable of inhibiting the adhesion and proliferation of C2C12 cells on their surfaces. These properties are advantageous for the potential application of the materials as stent coatings.

Keywords

Drug delivery, butyl rubber, coatings, stent, polyisobutylene

Introduction

Polyisobutylene (PIB) and its copolymers with small percentages of isoprene, commonly referred to as butyl rubber, are chemically stable and impermeable materials that are widely used in applications including vehicle tires, industrial sealants, chewing gum, and bladders for sporting equipment. A triblock copolymer of polystyrene (PS)-PIB-PS (SIBS) is used in the clinical Taxus vascular stent, where it serves as a coating for the physical incorporation of paclitaxel (PTX).[1-3] In this application, PTX serves as an anti-proliferative agent that prevents restenosis, the post-operative recurrance of arterial narrowing.[4, 5 6]

A variety of synthetic approaches have been developed for functionalizing the terminus of PIB with moieties such as halogens,[7, 8] thiols,[9] sulfonates,[10] amines,[7] silanes,[11] alcohols,[8, 12-15] olefins[16, 17] or carboxylic acids.[18-20] Alternatively, the isoprene units of butyl rubber provide alkenes along the polymer backbone and have served as functional handles for halogenation, cross-linking and other reactions.[21-27] While most of these reactions afford incomplete reactions

or mixtures of different products and isomers,[25, 26, 28-30] we have recently reported a clean and efficient epoxidation-elimination sequence for introducing allylic alcohol groups to the backbone.[31] These alcohol groups were activated and functionalized to prepare graft copolymers[31-33] and have also been further derivatized to afford carboxylic acid groups.[34] The carboxylic acid groups imparted increased tensile strength, which was proposed to result from cross-linking through hydrogen bonding,[24, 35, 36] as well as enhanced adhesion to stainless steel as a result of binding between the carboxylic acid groups and the metal surface.[34, 37-39] Building on this epoxidation-elimination sequence,[31] as well as work by Parent, Whitney, and coworkers,[29] the allylic alcohol moieties were also converted to *cis*-dienes and it was demonstrated that these dienes could undergo Diels-Alder reactions with maleic anhydride.[40] Reaction of the resulting anhydrides with alcohol- or amine-terminated poly(ethylene oxide) (PEO) or PS provided graft copolymers, while at the same time introducing carboxylic acid groups to the backbone.[40]

As described above, because of its favorable chemical and biological properties, PIB-based materials are of significant interest for application as coatings for drug-eluting stents.[1, 3] The current generation of stents incorporates physically encapsulated drug within a polymeric coating.[41, 42] While they reduce the risk of restenosis relative to bare metal stents,[43] there remains the risk of post-operative thrombosis due to the limited lifetime of the drug release.[6, 44-47] Another serious concern is the delamination of the polymer from the stent due to poor adhesion. Not only can this cause a burst-release of a highly toxic drug into the blood stream, it also can cause small pieces of polymer to circulate in the blood, potentially causing serious complications.[48, 49] Covalent immobilization of the drug has been proposed as a potential solution to lengthen the lifetime of the stent. Several examples involving the introduction of

drugs through functionalization of the polymer termini have been reported.[50-56] However, these drug loadings were generally very low compared to the commercial devices.

In recent work, our group ultilized carboxylic acid functionalized PIB, prepared through derivatization of the isoprene units in butyl rubber, to covalently immobilize PTX via ester linkages.[57] This resulted in conjugates with high drug loadings up to 50 wt%, depending on the isoprene content of the starting rubber. Slow drug release was obtained from coatings of these materials due to the requirement for ester hydrolysis to occur within the hydrophobic environment of the polymer prior to drug release. This approach was also extended to arborescent PIB with short terminal isoprene-rich domains.[58] Here we describe the use of a maleic anhydride Diels-Alder adduct of PIB (**PIB-MA**) derived from butyl rubber to simultaneously introduce PTX and carboxylic acids to the PIB backbone via ring-opening of the ahydride. The resulting polymer **PIB-PTX-COOH** offers the potential to concomitantly benefit from covalent drug attachment of PTX and the favorable mechanical and adhesive properties resulting from the carboxylic acid moieties. PS can also be introduced at the same time as PTX, to afford a PTX conjugate of a PIB-PS graft copolymer (**PIB-PS-PTX-COOH**). PTX release from coatings of these materials is reported and the tensile and adhesive properties are investigated and compared to the starting butyl rubber and SIBS. Preliminary biological studies are also described.

Experimental

General procedures and materials

Butyl rubber containing 2 mol% isoprene ($M_w = 3.39 \times 10^5$ g/mole, dispersity ($Đ$) = 2.2 relative to PS standards) was provided by LANXESS Inc. (London, Canada). **PIB-MA** was prepared

from butyl rubber as previously reported.[40] Solvents were purchased from Caledon Labs (Caledon, Ontario). PTX was purchased from LC laboratories (Woburn, Ma) or Ontario Research Chemicals (Guelph, ON). All other chemicals were purchased from either Sigma-Aldrich or Alfa Aesar and were used without further purification unless otherwise noted. Dry toluene was obtained from an Innovative Technology (Newburyport, USA) solvent purification system based on aluminium oxide columns. $CHCl_3$ and *N*,*N*-diisopropylethylamine (DIPEA) were freshly distilled from CaH_2 prior to use. ^{1}H NMR spectra were obtained in $CDCl_3$ at ~~600~~ 400 MHz on a Varian Inova instrument. NMR chemical shifts (δ) are reported in ppm and are calibrated against residual solvent signals of $CDCl_3$ (δ 7.26). Abbreviations used include: s, singlet; d, doublet; t, triplet; dd, doublet of doublets; td, triplet of doublets; q, quartet; m, multiplet; br, broad singlet. All coupling constants (*J*) are reported in Hz. Due to significant relaxation time differences, the integration of the backbone PIB resonances is not to scale with the integration of the isoprene-derived resonances attached to the PTX even with a d_1 of 10 s. This phenomenon was also observed with similar materials.[58, 59] Consequently, the extent of PTX coupling in **PIB-PTX-COOH** was evaluated from a comparison of the integrations of the signals at 8.14, assigned to PTX, and 5.50, assigned to unreacted **PIB-MA** cycloadduct. The details of the calculation are available in the supporting information (Figure S1). The PTX content of **PIB-PS-PTX-COOH** was calculated in a similar manner, while the PS content was evaluated from integrations of the signals at 7.30-6.86 ppm (belonging to the meta and para hydrogens of the phenyl groups of PS) and the signal 1.40 ppm belonging to -CH_2-of the polyisobutylene backbone. Details of this calculation are provided in the SI (Figure S2). Infrared spectra were obtained of polymer films from CH_2Cl_2 on NaCl plates using a Bruker Tensor 27 instrument. Differential scanning calorimetry (DSC) and thermogravimetric analysis (TGA) were performed

on a TA Q20 DSC machine and a TA Q600 SDT machine respectively. For DSC, the heating/cooling rate was 10 °C/min between -120 to +150 °C. Glass transition temperatures (T_g) were obtained from the second heating cycle. Thermal data was interpreted using Universal Analyses 2000 (TA Instruments).

Synthesis of PIB-PTX-COOH

To a solution of PTX (1.9 g, 2.2 mmol, 5 equiv.), 4-dimethylaminopyridine (DMAP) (78 mg, 0.62 mmol, 1.5 equiv.) and DIPEA (3.7 mL, 21 mmol, 46 equiv) in anhydrous $CHCl_3$ (125 mL), **PIB-MA**[40] (2.0 g, 0.52 mmol of anhydride, 1.0 equiv), cut into small pieces no more than 4 mm in any dimension, was added as a solid. The reaction mixture was heated at reflux under argon with stirring for 72 hours, then cooled to room temperature, decanted to remove material that formed a gel on the side of the flask, and precipitated dropwise into acetone (final ratio of 3:1 acetone:$CHCl_3$). The solid was then redissolved in $CHCl_3$, acidified with trifluoroacetic acid (200 µL, 2.6 mmol), and re-precipitated to ensure the removal of all unreacted PTX (the combined ~~s~~supernatants from the precipitations were concentrated and purified by column chromatography using 9:1 acetone:hexanes as an eluent to recover the unreacted PTX in >98 % purity for reuse). The resulting **PIB-PTX-COOH** was triturated with three 50 mL portions of acetone, and then dried *in vacuo* to provide 1.8 g of the product as an amorphous viscoelastic white solid in 76 % yield. ^{1}H NMR indicated 88% maleic anhydride ring opening by PTX (Figure S1) corresponding to 21 wt% PTX in the product. ^{1}H NMR (~~600~~ 400 MHz, $CDCl_3$): δ_{ppm} 8.15 (d, *J* = 7.7 Hz, 1H), 7.85 (d, *J* = 7.7 Hz, 1H), 7.40-7.63 (m, 7H), 7.17 (br s, 1H), 6.98-6.90 (m, 1H), 6.30-6.15 (m, 2H), 6.06 (dd, *J* = 15.0, 11.0 Hz, 1H), 5.96 (dd, *J* = 13.0, 13.0 Hz, 1H), 5.76 (dd, 5.47 *J* = 8.8, 8.8 Hz, 1H), 5.69-5.59 (m, 2H), 5.27-5.22 (m, 2H), 4.93-4.85 (m, 1H), 4.85-4.65 (m, 1H), 4.48-4.37 (m, 1H), 4.30-4.05 (m, 4H), 3.13-3.00 (m, 4H), 2.60-2.50 (m, 4H),

2.40 (s, 3H), 2.30 (s, 5H), 2.05-1.95 (m, 10H), 1.82 (s, 3H), 1.40 (s, 1142H), 1.09 (s, 3190H). IR (thin film, NaCl) ν_{max}: 3220, 2985, 2734, 1942, 1922, 1868, 1844, 1829, 1791, 1772, 1734, 1716, 1684, 1669, 1652, 1647, 1636, 1617, 1576, 1569, 1558, 1540, 1521, 1506, 1472, 1389, 1366, 1230, 737. T_g = -64 °C.

Synthesis of PIB-PS-PTX-COOH

The same procedure as that described above for the preparation of **PIB-PTX-COOH** was used except for the following changes to reagent amounts: PTX (1.6 g, 1.9 mmol, 4 equiv.); DMAP (61 mg, 0.50 mmol, 1.0 equiv.); DIPEA (1.7 mL, 10 mmol, 20 equiv); hydroxyl-terminated PS (M_n = 4-5 kDa, 1.1g, 0.25 mmol, 0.5 equiv.); anhydrous $CHCl_3$ (150 mL); **PIB-MA**^{40} (1.9 g, 0.50 mmol of anhydride, 1.0 equiv). This provided 2.4 g of a white solid after removal from any gelled material and two precipitations (72 % yield). ^{1}H NMR indicated 42% maleic anhydride ring opening by PTX (Figure S2) corresponding to 10 wt% PTX content and 9% ring opening by PS (Figure S2), corresponding to 12 wt% PS in the product. ^{1}H NMR (~~600~~ 400 MHz, $CDCl_3$): δ_{ppm} 8.19-8.14 (m, 1H), 7.36-7.56 (m, 6H), 7.30-6.80 (m, 213H), 6.80-6.25 (m, 139H), 5.97 (s, 1H), 5.93 (s, 1H), 5.55-5.51 (m, 2H), 5.39 (s, 2H), 5.36-5.30 (m, 1H), 5.26-5.18 (m, 2H), 5.10-4.80 (m, 1H), 4.18 (m, 2H), 3.75-3.60 (m, 0.5H), 3.42-3.25 (m, 6H), 3.20-3.09 (m, 1H), 3.00-2.85 (m, 1H), 2.60-2.40 (m, 3H), 2.25-1.60 (m, 182H), 1.41 (s, 1645H), 1.09 (s, 4724H). IR (thin film, NaCl) ν_{max}: 3220, 3082, 3059, 2952, 2734, 1780, 1734, 1716, 1652, 1647, 1636, 1601, 1558, 1541, 1521, 1506, 1472, 1389, 1366, 1261, 1230, 802, 758, 737, 700 cm^{-1}. T_g = -63 and 87 °C.

Tensile testing

Tensile tests were performed according to ASTM D882 – 12^{60} using an Instron 3365 Universal Testing Machine. For each sample, 1.5 g of polymer was compressed into 0.3 mm thick flat

sheets using a hydraulic hot press (Carver Hydraulic Unit Model # 3851 OC). Samples 60 mm × 5mm in size were cut from this sheet for analysis. The tensile test was performed using a 1 kN load cell and an extension rate of 400 mm/min at ambient temperature (22 ± 1 ºC). Load and extension calibration were preformed prior to the test. To prevent slippage of the samples from the clamps, 10 mm of material was inserted into each clamp giving an effective length of 40 mm. At least six trials were performed for each polymer.

Adhesion testing

Adhesion tests were performed according to ASTM D1002 using an Instron 3365 Universal Testing Machine. For each sample, 20 mg of polymer was dissolved in 20 mL of $CHCl_3$. 5 mL of each sample was drop-cast onto a polished 50 mm x 25 mm stainless steel 316L plate. A second plate was placed on top of the applied area and left to dry under vacuum. The adhesion test was performed using a 1 kN load cell and an extension rate of 1 mm/min at ambient temperature (22 ± 1 ºC). Load and extension calibration were preformed prior to the test. To prevent slippage of the samples from the clamps, 10 mm of plate was inserted into each clamp leaving only applied area (1000 mm^2) between the clamps. At least three trials were performed for each polymer.

Preparation of coatings

The surface of a stainless steel plate (stainless steel 316L) with dimensions of 31 mm × 11 mm was made smooth with a bench-top polisher. The films were prepared from a 100 mg/mL solution of the polymer in CH_2Cl_2. For the physically mixed samples, PTX was added to achieve the desired weight percentage. A 100 μL aliquot of solution was drop cast onto the stainless steel plate. The sample was dried under reduced pressure prior to the release study. Each sample was prepared and studied in quadruplicate.

Atomic force microscopy

Surfaces for AFM analysis were those prepared for the release study described above. They were visualized using an XE-100 microscope from Park Systems. Images were obtained by scanning the surface at three different resolutions: 20 μm × 20 μm, 5 μm × 5 μm, and 1 μm × 1 μm. Scanning was carried out using rectangular-shaped silicon cantilevers (T300, VISTA probes), with a nominal tip radius of 10 nm and spring constant of 40 N/m. Measurements were carried out under atmospheric conditions and ambient temperature. Topographic (height) and phase (force imaging mode) images were recorded simultaneously in tapping mode. The cantilever was oscillated at its resonance frequency of approximately 300 kHz. All images contained 256 data points per line for 256 lines, and the scan rate was maintained at 1 Hz. Post-imaging analysis was performed using XEI, version 1.7.0 from Park Systems. Images were flattened to remove curvature in both the x and y axes.

PTX release study

The release study was performed in pH 7.4, 0.01 M phosphate buffer containing 0.138 M NaCl and 0.0027 M KCl and 0.05% (m/v) Tween 20 as a surfactant. The polymer-coated stainless steel plates were submerged in 10 mL of buffered solution in a vial. The solution was maintained at 37 °C. The buffer was removed every seven days for PTX analysis and replaced with fresh medium. Due to the low amounts of PTX released, the release medium was removed via lyophilization and the resulting solid redissolved in 2 mL of 80:20 water:acetonitrile and filtered through a 2.2 μm syringe filter. A control study demonstrated that PTX was soluble at this concentration. HPLC analysis was performed as previously reported.[57]

Toxicity assay

Sample preparation: Test samples were melt-pressed to a thickness of 0.4 mm using a hot press (Carver Hydraulic Unit Model # 3851 OC). The melt-pressed film was then cut into 1 cm × 1 cm

squares. Samples were sterilized by washing with 70% ethanol and subsequently dried for 2 hours under UV light. They were placed in Petri dishes and incubated in 2 mL of Dulbecco's Modified Eagle Medium (DMEM, Invitrogen) supplemented with 10% fetal bovine serum (Invitrogen), 1% Glutamax (100x) solution and 1% Penstrep (100x) in an incubator at 37 °C for 24 hours. The leachate was then removed and passed through a 0.2 µm filter.

MTT assay: C2C12 mouse myoblast cells were seeded in a Nunclon® 96-well U bottom transparent polystrol plate to obtain 10,000 cells/well in 100 µL of the DMEM containing serum, glutamax and antibiotics as described above. The cells were allowed to adhere to the plate in a 5% CO_2 incubator at 37 °C for 24 hours. Next, the growth medium was aspirated and was replaced with either the positive control sodium dodecyl sulfate (SDS) in the cell culture medium at concentrations of 0.2, 0.15, 0.10, or 0.05 mg/mL, serial two-fold dilutions of the leachate, or just the medium. The cells were then incubated at 37 °C (5% CO_2) for 24 hours. The medium was then aspirated and replaced with 110 µL of fresh medium containing 0.5 mg/mL (3-(4,5-dimethylthiazol-2-yl)-2,5-diphenyltetrazolium bromide) (MTT) reagent. After 4 hours of incubation (37 °C, 5% CO_2), the MTT solution was carefully aspirated and the purple crystals were dissolved by addition of 50 µL of spectroscopic grade dimethylsulfoxide (DMSO). After shaking (1 second, 2 mm amp, 654 rpm), the absorbance of the wells at 540 nm was read using an M1000-Pro plate reader (Tecan). The absorbance of wells not containing cells but treated by the above steps was subtracted as a background and the cell viability was calculated relative to wells containing cells that were exposed to just culture medium. No (0%) cell viability was detected for the cells exposed to the highest concentrations of the positive control SDS, confirming the sensitivity of the assay.

Evaluation of cell growth on films

C2C12 cells were maintained at 37 ºC and 5% CO_2 in Dulbecco's Modified Eagle Medium (Invitrogen) supplemented with 10% fetal bovine serum (Invitrogen) and supplemented with 1% Glutamax (100x) solution and 1% Penstrep (100x). First, microscope glass cover slips (circular, 25 mm diameter) were coated with a minimum layer of polymer by drop casting a 35 mg/mL solution of polymer in toluene and allowing the solvent to dry completely. The surfaces were sterilized by submersion in 70% ethanol, and were then left to dry completely under reduced pressure for 96 hours. The sterilized samples were placed in the wells of a 6-well plate and 5×10^5 cells in 2 mL of cell culture medium were seeded onto each surface. The samples were incubated for 48 hours, then fixed with 4% paraformaldehyde solution for 10 min. The samples were washed twice with phosphate-buffered saline (PBS) (Invitrogen) at pH 7.2, and then treated with 2 mL of acetone at -20 ºC for 5 minutes to permeabilize the membrane. After that, they were washed again with PBS, and then stained with Alexa Fluor 568 phalloidin (Invitrogen) and DAPI (Invitrogen) following the manufacturer's directions. The samples were washed again with PBS and placed face down onto glass microscope slides with ProLong® Gold Antifade Reagent (Invitrogen) and sealed. Confocal images were obtained using a confocal laser scanning microscope (LSM 510 Duo Vario, Carl Zeiss) using a 20× objective and excitation wavelengths of 405 (DAPI) and 578 nm (phalloidin). Cells were counted using Image Pro Plus software on 5 different images per sample. Statistical analyses (ANOVA followed by Tukey's test) were performed using the software Excel.

Results and Discussion

Synthesis and characterization of PTX conjugates

PIB-MA was prepared as previously reported.[40] Briefly, as shown in Scheme 1A, butyl rubber containing 2 mol% of isoprene units was epoxidized to afford **PIB-EPOX**,[31] and the epoxide was opened with HCl in $CHCl_3$.[40] The resulting allylic alcohol **PIB-OH** was activated by treatment with methanesulfonyl chloride in the presence of K_2CO_3 and NEt_3 to provide **PIB-OMs**. Heating the mesylate (**PIB-OMs**) in the presence of DIPEA provided *exo*-diene **PIB-DIENE**, which underwent a Diels-Alder reaction at ambient temperature with maleic anhydride to afford **PIB-MA**.[40] The opening of these anhydrides with PTX was then investigated (Scheme 1B). Although PTX has two secondary hydroxyl groups, it has been well documented that the 2' hydroxyl is significantly more reactive and undergoes conjugation reactions, while the 7 hydroxyl group is reported as largely unreactive.[61, 62] Nucleophilic ring opening of the anhydride with 2.5 equiv. of PTX in refluxing $CHCl_3$ resulted in the formation of a large amount of gel, with little soluble material remaining after 3 days. The presence of the gel could be due to ionomeric or hydrogen-bond mediated cross-linking between the newly unmasked carboxylic acids or due to chemical cross-linking. The considerable steric demands on the PTX hydroxyl group may slow the reaction sufficiently to make the newly formed carboxylic acids on the polymer competitive nucleophiles while the possibility of PTX mediated cross-linking must also be considered as the free 7 hydroxyl group of a conjugated drug residue, although less reactive than the anchored 2' OH, could be responsible for ring-opening an additional anhydride leading to the formation of a network. Gel formation was also previously observed when hydroxyl-terminated PEO was reacted with **PIB-MA** under similar conditions.[40] However, increasing the PTX excess to 5 equiv. greatly suppressed the gel formation and provided the first target conjugate **PIB-PTX-COOH**.

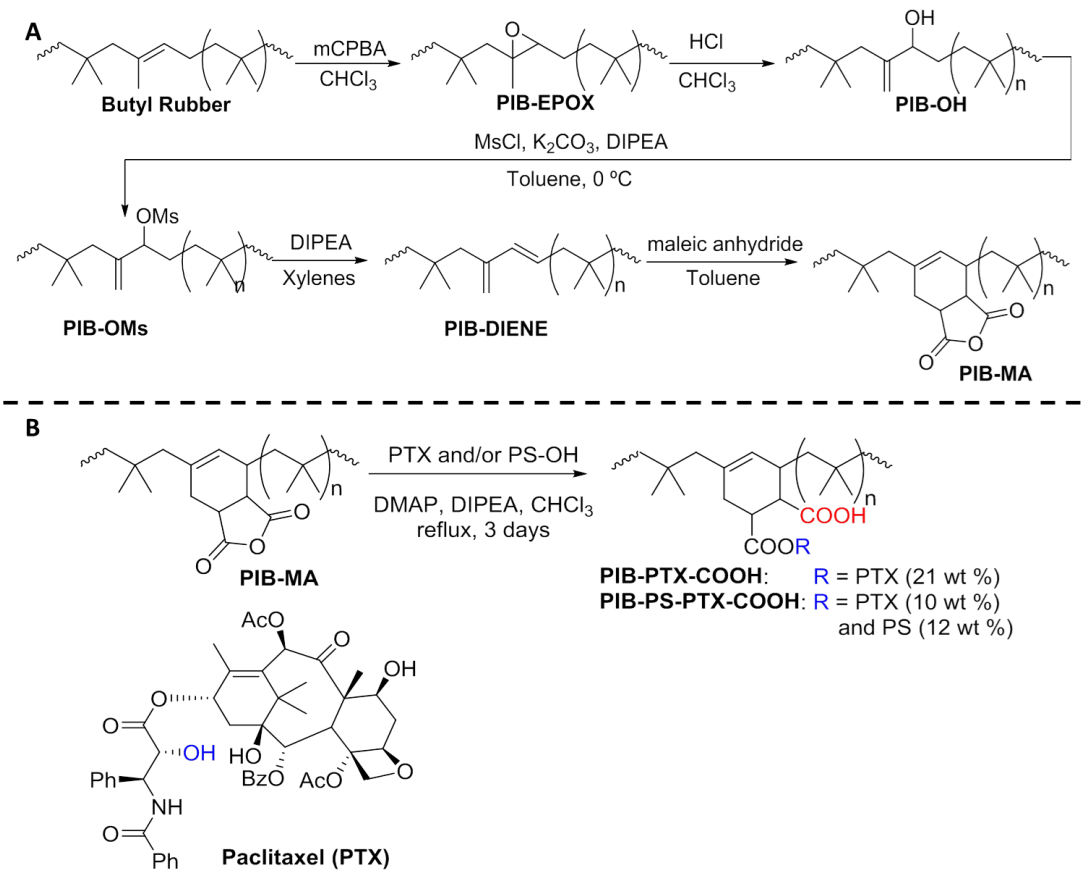

Scheme 1. A) Synthesis of **PIB-MA** from **Butyl Rubber**. This synthesis has been described previously.[40] **B)** Synthesis of graft copolymers **PIB-PTX-COOH**, **PIB-PS-PTX-COOH** and the structure of paclitaxel (PTX). The labeled 2' hydroxyl is the site of conjugation.

Based on ^{1}H NMR spectroscopy (Figure S1), approximately 88% of the anhydride groups on the polymer were opened by PTX, resulting in **PIB-PTX-COOH** having a PTX content of 21 wt%. The spectral integration of these side chains is not quantitative with respect to the peaks corresponding to the isobutylene units along the polymer backbone. We have previously observed this same effect with arborescent rubber-PTX graft copolymers, presumably because the nuclei on the pendant groups do not relax on the same timeframe as the backbone (even with a d_1 of 10 s).[58] Consequently, the conversion was determined by comparing the integration of the

PTX peaks with those derived from the maleic anhydride groups. IR spectroscopy confirmed the successful coupling as the peak at 1780 cm^{-1}, characteristic of the carbonyl on the anhydride, could no longer be detected (Figure S3). New bands at 1734 and 1716 cm^{-1} appeared. This suggests a high conversion of the anhydride to a product containing new carbonyls such as those from the resulting ester and acid of the conjugate along with those present in PTX. The spectrum is consistent with those previously observed for PTX-PIB constructs.[57, 58] Unfortunately size exclusion chromatography (SEC) analysis was not possible due to undesirable interactions of the pendant carboxylic acid groups with the SEC column. The thermal properties of the new materials are summarized in Table 1 and the data is included in the supporting information (Figures S5-S8). The T_g for **PIB-PTX-COOH** was -64 °C, quite similar to the T_g range of -70 to -63 °C reported for butyl rubber.[63, 64] Despite PTX being a semicrystalline solid with a melting point of 216-217 ºC, no T_m was observed for this conjugate. This suggests that PTX is homogeneously distributed throughout the material, rather than existing in phase-separated domains. This is consistent with our previous results for linear PIB-PTX conjugates.[57] The onset degradation temperature (T_o) for **PIB-PTX-COOH** was 369 ºC and the peak degradation temperature (T_p) was 413 ºC, similar to butyl rubber. While PTX is known to decompose at ~213 ºC, its incorporation into the polymer seems to increase its thermal stability. This was also observed for linear conjugates containing homogeneously distributed PTX,[57] whereas arborescent analogues with phase-separated PTX domains (based on DSC), exhibited a two-phase decomposition with the first phase corresponding to PTX degradation.[58]

Table 1. Thermal properties of the PTX conjugates as measured by DSC and TGA.

Polymer	T_g (ºC)	T_o (ºC)	T_p (ºC)
PIB-PTX-COOH	-64	369	413
PIB-PS-PTX-COOH	-63, 87	374	415

As previously reported, **PIB-MA** can also be opened by hydroxyl-terminated polymers such as PS (PS-OH) and PEO.[40] While PIB-PEO graft copolymers have been extensively reported by our group and others,[28-30, 32, 59, 65, 66] PS was of particular interest due to the use of SIBS in stent coatings. Linear block copolymers of PIB with PS or polyalloocimene have been found to exhibit thermoplastic elastomeric (TPE) properties that are conducive to their application in stent coatings.[67-69] The current synthetic approach offers the possibility to prepare PIB-PS graft copolymers also incorporating covalent PTX for controlled release and carboxylic acids for enhanced metal adhesion. The target **PIB-PS-PTX-COOH** graft copolymer was prepared by ring opening of **PIB-MA** with PS-OH (4000-5000 g/mol) (0.5 equiv.) and PTX (4 equiv.). ^{1}H NMR spectroscopic analysis suggested that 9% of the anhydrides were opened by PS and 42% were opened by PTX, providing 12 wt% of PS and 10 wt% of PTX (Figure S2). The IR spectrum of **PIB-PS-PTX-COOH** was similar to that of **PIB-PTX-COOH** except that it also showed a peak at 1600 cm^{-1}, which can be attributed to the monosubstituted benzene moiety in PS and the anhydride peak at 1780 cm^{-1} had not entirely disappeared, consistent with the ring opening of only ~50% of the anhydrides (Figure S4). Furthermore, peaks 800, 757, and 700 cm^{-1} characteristic of PS were also observed. **PIB-PS-PTX-COOH** had a T_g of -63 °C corresponding to PIB, but also a T_g of 87 °C due to the PS, suggesting that these blocks exist in phase-separated

domains. T_o and T_p were 374 and 415 °C respectively, very similar to those observed for **PIB-PTX-COOH**.

Preparation and study of PTX-eluting coatings

Coatings of **PIB-PTX-COOH** and **PIB-PS-PTX-COOH** were prepared by dissolving the polymer in toluene and dropcasting it onto 316L stainless steel substrates. Coatings of controls comprising SIBS (30 wt% PS) with physically encapsulated PTX, either 8.8 wt% as used in the clinical formulation or 24 wt%, similar to **PIB-PTX-COOH**, were also prepared and studied in our previous report[57] and the data is included here for comparison purposes. Drug release was studied using a previously reported procedure[57, 70-72] involving the immersion of coated slides in pH 7.4, 0.01 M phosphate buffer containing 0.138 M NaCl, 0.0027 M KCl, and 0.05% (m/v) Tween 20 as a surfactant.[57] PTX released from the slides into the solution was quantified by HPLC. As shown in Figure 1, the physical mixtures of PTX and SIBS released 0.6 to 1.2 % of the drug over 35 days, depending on the PTX loading.[57] **PIB-PTX-COOH** released 0.4% of its PTX over the same period and **PIB-PS-PTX-COOH** released 0.13%. This slower release from the covalent conjugates can be attributed to the requirement for ester hydrolysis to occur prior to PTX release rather than simple diffusion from the physical mixtures. The surrounding polymer provides a very hydrophobic environment, where ester hydrolysis would be slow. Slow PTX release may offer advantages in terms of increasing the drug-eluting lifetime of the stent, thereby preventing restenosis over the longer term. However, this release is faster than that observed for our previous covalent conjugates where release was less than 0.1% of the loaded drug over the same time period.[57] This can likely be attributed to the presence of the carboxylic acid groups,

which increase the polarity of the polymer and enable increased water penetration into the coating.

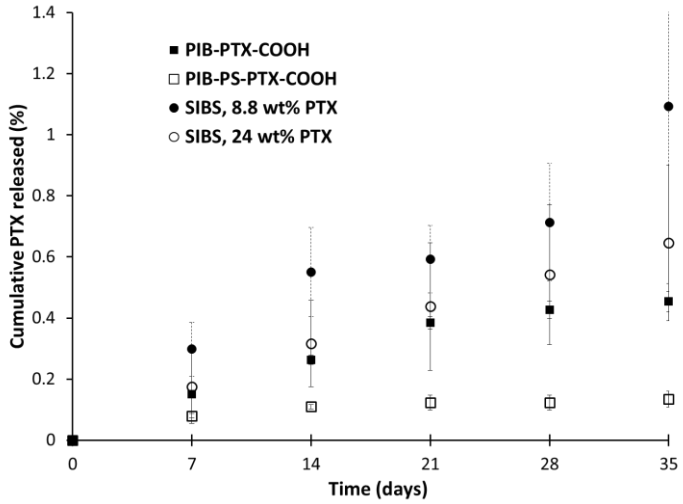

Figure 1. Release of PTX from **PIB-PTX-COOH** and **PIB-PS-PTX-COOH** compared to previously reported release profiles of physical mixtures of PTX (8.8 or 24 wt%) from SIBS (30% PS).[34]

The coatings were also studied by AFM before and after the release study. The behaviour of the materials is completely consistent with what we have previously observed for other PTX-PIB covalent conjugates.[57, 58] There is no observed phase separation of either the PTX or PS domains indicating that the material is relatively homogenous on the surface. Unlike for physical mixtures, the surface does not appreciably roughen for these covalent conjugates over the 35-day release study. The AFM images, and a further discussion including references is included in the SI (Figure S9).~~As shown in Figures 2A and 2B, prior to the release, **PIB-PTX-COOH** exhibited only rippling features on the order of 10 – 20 nm in height, characteristic of butyl rubber rippling that we have previously observed.[32, 57, 58] No discrete PTX domains were observed. **PIB-PS-**~~

PTX-COOH exhibited similar rippling but also some hills with lateral dimensions on the order of a few micrometers and heights of 50-75 nm (Figure 2D and 2E). These could possibly be domains of PTX, but the thermal properties of the polymers did not suggest phase separation of PTX and the scale of the features is too large for phase separation of a covalent copolymer system. There is no clear indication from the phase image that the hills differ in composition from the rest of the material. No distinct PS domains were observed at this magnification or at 20-fold higher (Figure S12). The phase separation of PS from PIB typically observed in SIBS is a result of annealing at 115 ºC.[73-75] As previously reported, coatings of SIBS containing physically incorporated PTX exhibited hill-like features characteristic of phase-separated PTX.[57, 58, 70, 76, 77] Images of the coating containing 8.8 wt% PTX are provided in Figure 2G and 2H, and images of SIBS with 24 wt% PTX can be found in the previous report.[57] After 35 days of PTX release, no significant changes in the surface were observed for **PIB-PTX-COOH** (Figure 2C). **PIB-PS-PTX-COOH** exhibited increased surface roughness after PTX release and the hill-like features were replaced by holes (Figure 2F). This may be attributable to the release of PTX from the coating or some other morphological rearrangement of the polymer. As previously noted by our group and others, after 35 days of PTX release, the distinctive PTX domains from the physical mixture of SIBS and PTX disappeared and were replaced by holes (Figure 2I).[57, 58, 76]

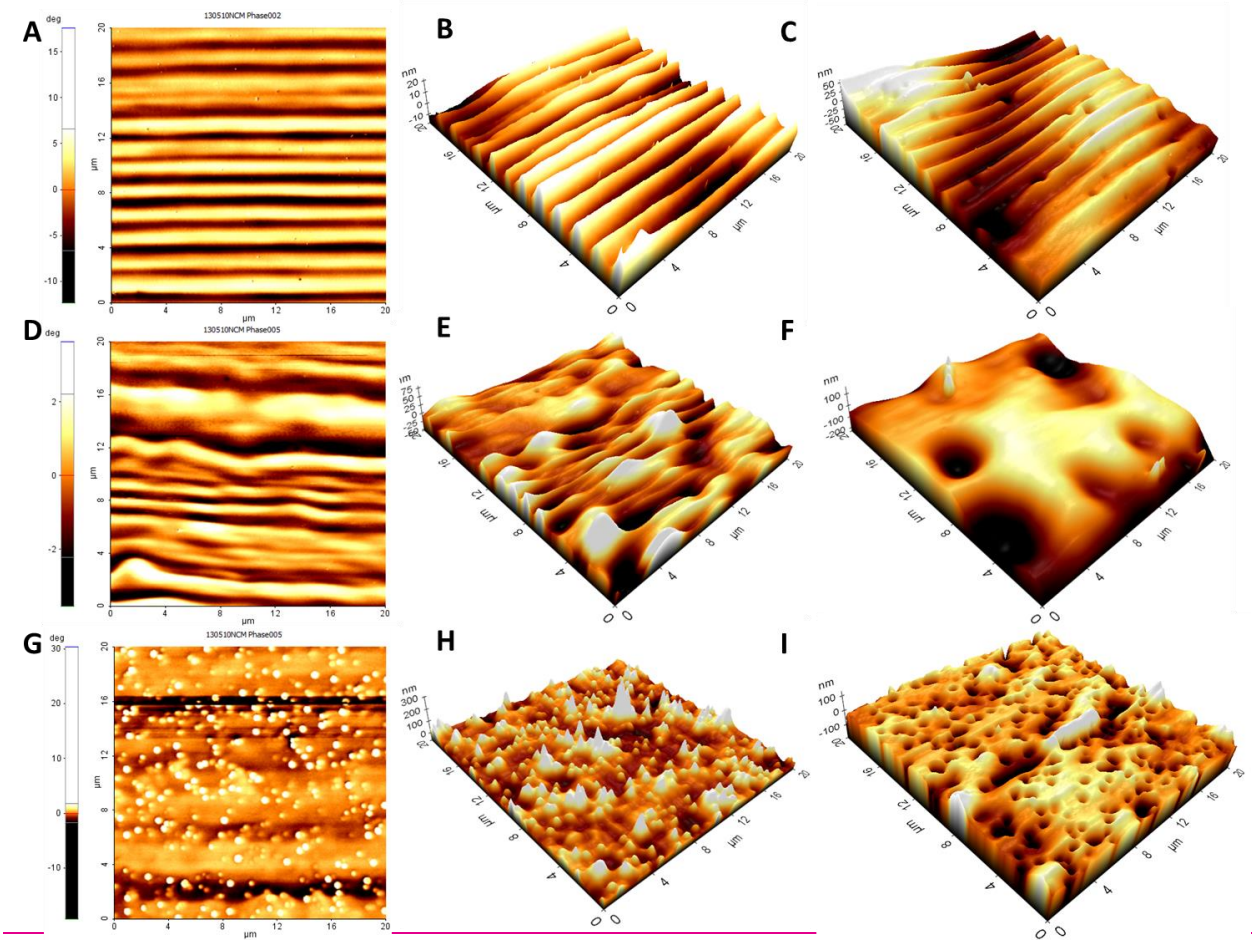

~~**Figure 2**: AFM images (20 µm x 20 µm) showing the polymer surface before and after the release study. A-C) **PIB-PTX-COOH**; D-F) **PIB-PS-PTX-COOH**; G-H) SIBS with 8.8 % PTX as a physical mixture. Phase images before release: A, D, G; topography images before PTX release: B, E, H; topography images after 35 days of PTX release: C, F, I. Phase diagrams for the samples after release are present in the SI, Figures S9-S11.~~

Mechanical and adhesive properties of the polymers

The tensile properties of polymers employed in stent coatings are also important, as the coatings must withstand the process of stent expansion. Tensile testing was performed to evaluate the ~~Young's modulus~~elastic modulus, ultimate tensile strength, and elongation at break for the

conjugates. The properties of the starting butyl rubber as previously reported are also included for comparison.[34] Representative stress-stain curves are shown in Figure 3 and the results are summarized in Table 2. The ~~Young's~~ elastic modulus, represented by the secant modulus measurement (stress at 5% strain) of **PIB-PTX-COOH** (~~0.6 MPa~~60 Pa) was ~~the~~ similar ~~same as~~to that of butyl rubber. This is consistent with previous results for PIB with similar percentages of pendant carboxylic acids, whereas higher amounts of carboxylic acids tended to increase the modulus.[34] The incorporation of PS in **PIB-PS-PTX-COOH** resulted in a ~~–~~similar ~~reduced~~ modulus of ~~0.4~~40 ~~M~~Pa, suggesting that the incorporation of polystyrene at this level provides little change in the tensile behaviour of the material and all are behaving as elastic as butyl rubber. ~~Polystyrene itself has a modulus of approximately 3300 MPa,[73] and the copolymer could be expected to become more rigid with the incorporation of 12 weight percent polystyrene; however, it appears this is not a sufficient amount of polystyrene to influence the elastic modulus.~~ Both **PIB-PTX-COOH** and **PIB-PS-PTX-COOH** have ultimate tensile strengths of ~2 MPa, approximately 10-fold higher than that of butyl rubber. This was expected as in previous work carboxylic acids,[34] PTX,[57, 58] and PS[40] were each independently found to increase the tensile strength of butyl rubber. Despite the increase in tensile strength, the elongation at break was similar for butyl rubber and the functionalized derivatives, ranging from 770 to 900%. Overall, the tensile strength and Young's moduli of these conjugates were lower than that of SIBS.[74] However, they might be enhanced by the incorporation of larger factions of the moieties by starting with butyl rubber with higher isoprene content.[34, 40]

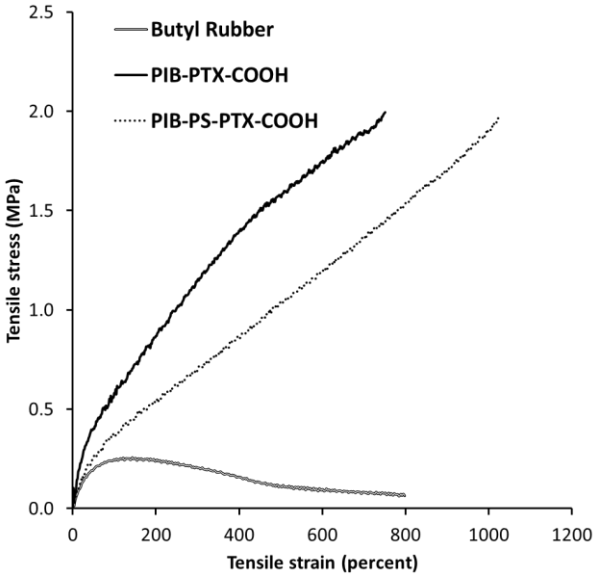

Figure 3. Representative stress-strain curves for butyl rubber, **PIB-PTX-COOH**, and **PIB-PS-PTX-COOH**.

Table 2. Summary of the tensile properties of butyl rubber, **PIB-PTX-COOH**, and **PIB-PS-PTX-COOH**.

	~~Young's modulus~~Secant modulus at 5% strain (~~M~~Pa)	Ultimate tensile strength (MPa)	Elongation at break (%)
Butyl Rubber (2 mol% isoprene)	~~0.6 ± 0.2~~40 ± 10	0.23 ± 0.01	770 ± 70
PIB-PTX-COOH	~~0.6 ± 0.1~~60 ± 20	2.0 ± 0.2	770 ± 80
PIB-PS-PTX-COOH	~~0.4 ± 0.1~~40 ± 10	1.9 ± 0.4	900 ± 200

A primary reason for incorporating carboxylic acid groups was to enhance the adhesion of the materials to the surface of the metal stent in order to prevent coating delamination. It was previously shown that the introduction of carboxylic acids or other ionomeric functionalities

improved the adhesion of materials to stainless steel.[34, 75, 76] This was investigated for **PIB-PTX-COOH** and **PIB-PS-PTX-COOH** in comparison with butyl rubber using ASTM test D1002. Briefly, this test involved the preparation of coatings of these materials between two stainless steel plates. A Universal Testing Machine was then used to measure the force required to separate the two plates. As shown in Table 3, 15 psi was required for the PIB coating. **PIB-PTX-COOH** required a nearly 4-fold higher force of 55 psi, while **PIB-PS-PTX-COOH** required 5-fold higher force to separate the plates. These results suggest that carboxylic acids do indeed provide enhanced adhesion and that the PS may also impart an increase in adhesion to stainless steel. Consistent with these results, in the release study described above, coatings of the covalent conjugates did not show any signs of delamination after the release, indicating strong adhesion to stainless steel and minimal disruption to the coating upon PTX release (Figure 4). On the other hand, the SIBS coating (30% PS) containing 8.8 wt% PTX rapidly delaminated from the stainless steel and developed holes and other imperfections in the coating. This is consistent with reports suggesting the poor adhesion of SIBS materials to steel substrates.[77]

Table 3. Adhesion properties of the butyl rubber samples, error represents the standard deviation of three measurements.

Material	Force/unit area required to separate (psi)
Butyl rubber (2 mol% isoprene)	15 ± 2
PIB-PTX-COOH	55 ± 10

PIB-PS-PTX-COOH	76 ± 11

Figure 4. Digital images of the films after release study: A) **PIB-PTX-COOH**; B) **PIB-PS-PTX-COOH**; C) SIBS with 8.8 wt% PTX.

Preliminary *in vitro* assessment of the coatings

Given the slow release of PTX from the covalent conjugates, it was of interest to determine whether the coatings released toxic levels of PTX and whether they supported the growth of cells on their surfaces. The widely used C2C12 mouse myoblast cell line was selected as a model cell line for these studies. The polymers are not soluble in aqueous solution, but the leaching of toxic species from the materials was evaluated by incubating coatings of the polymers in cell culture medium, and then adding this medium to C2C12 cells in serial 2-fold dilutions. An MTT assay was carried out to assess the viabilities of cells grown in this leachate.[78] As shown in Figure 5, all dilutions of leachate from **PIB-MA**, **PIB-PTX-COOH**, and **PIB-PS-PTX-COOH** afforded greater than 70% cell viability, similar to that of the negative (non-toxic) control HDPE. Based on the benchmark of 70% viability indicated by this ISO 10993-5 protocol, these materials can be deemed to not release toxic compounds.[79] A physical mixture of SIBS (with 30 % polystyrene by weight) containing 24 wt% PTX was also studied for comparison. All leachate dilutions

resulted in greater than 70% viability and there is no statistical difference between any of the samples at the higher leachate levels, but at 25 % leachate, the SIBS-PTX sample with the physically encapsulated PTX (24 wt %) was more toxic than any of the other materials (**PIB-MA, PIB-PTX-COOH, PIB-PS-PTX-COOH** and **HDPE**) at the $p < 0.05$ level as determined by ANOVA and paired post-hoc Tukey's tests. Overall, these results suggest that coatings of the covalent conjugates do not release toxic levels of PTX. This can likely be attributed to the very slow release of PTX which does not allow PTX to reach cytotoxic concentrations during the 24 h incubation in cell culture medium.

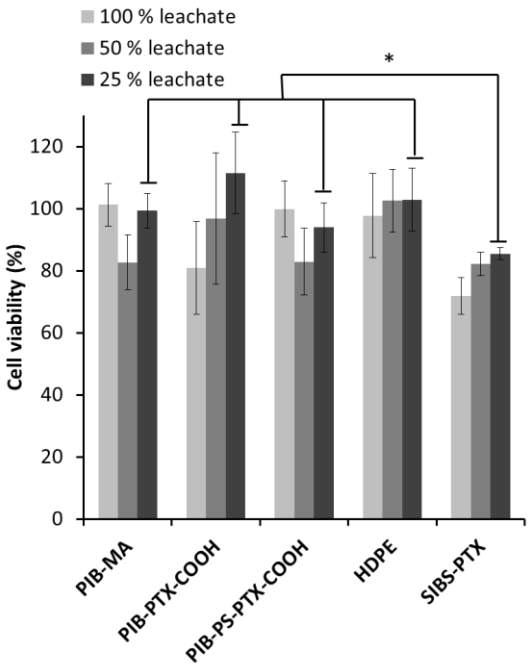

Figure 5. Viability of C2C12 mouse myoblast cells grown in various dilutions of leachate (cell culture medium that was incubated in the presence of polymeric materials) as measured by an MTT assay. Error bars represent the standard deviation of six measurements. * indicates that **SIBS-PTX** at 25 % leachate is statistically more toxic at the $p < 0.05$ level than the other samples (which have statistically undifferentiated means at this power level) using an ANOVA

and a post-hoc Tukey test. Note however, that at 80 % cell viability, according to ISO 10993-5, this material is still considered non-toxic.

Given the sub-toxic levels of PTX observed in the MTT assay described above, the ability of PTX to prevent the growth of cells associated with restenosis, particularly in the covalently conjugated systems, may be of concern. To investigate this, the growth of cells on surfaces of **PIB-PTX-COOH** and **PIB-PS-PTX-COOH** was studied and compared to glass, a good substrate for cell growth, and to butyl rubber. The polymers were coated on glass slides, seeded with C2C12 cells, incubated for 48 hours, and then washed to remove non-adherent cells. The cell nuclei were then stained with 4',6-diamidino-2-phenylindole (DAPI, blue) and the cytoskeletons with Alexa Fluor 568 phalloidin (green). The cells then were imaged by fluorescence confocal microscopy. As shown in Figure 6A and D, both the control glass and butyl rubber[57] support large numbers of live, healthy cells with normal cytoskeletons over the entire surface of the material. On the other hand, healthy cells were not detected on coatings of either **PIB-PTX-COOH** or **PIB-PS-PTX-COOH** (Figure 6B-D). There were regions where nuclei were observed, but without the elongated, healthy appearance of cells on the control surfaces. Instead, the few observed cells grew in clusters, indicative of their preference for one another compared to the surface. By counting the number of cells per mm^2, it was found that there was no significant difference in the number of cells found on glass versus butyl rubber. However, 120-fold fewer cells were observed on **PIB-PTX-COOH** and 260-fold fewer on **PIB-PS-PTX-COOH** relative to butyl rubber. These results are consistent with our observations for other linear[57] and arborescent PIB-PTX[58] conjugates without pendant carboxylic acids and suggest that despite the very slow release of PTX, these materials are also still able to prevent the growth of cells on their surfaces, a key aspect of their potential ability to prevent restenosis.

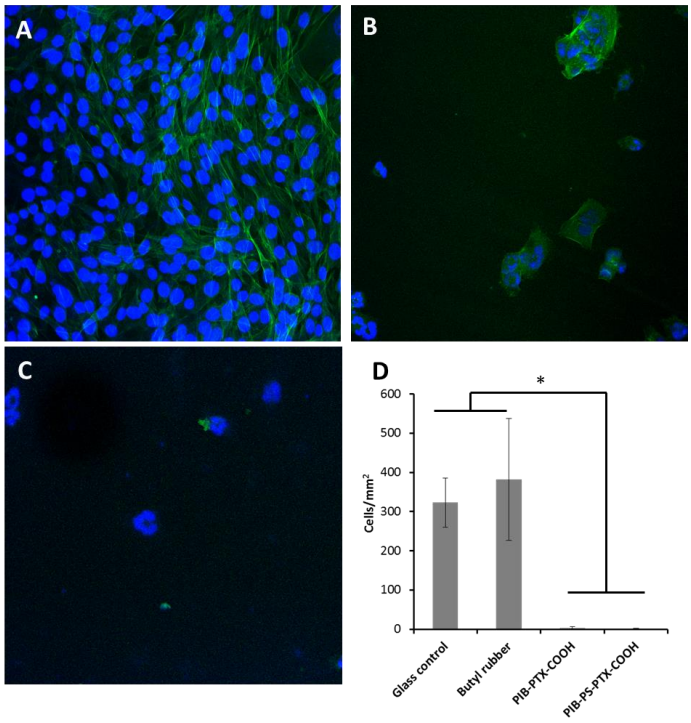

Figure 6. Confocal microscopy images of C2C12 cells on: A) glass slide control; B) **PIB-PTX-COOH**; C) **PIB-PS-PTX-COOH**; and D) Cell counts for the polymers examined (* indicates that the two controls are statistically different from the two treatments by ANOVA and Tukey's *post hoc* test; $p < 0.05$). Blue colour is due to DAPI that is selective for nuclear material, while the green colour is due to Alexa Fluor which binds selectively to cytoskeletons.

Conclusions

Using a maleic acid adduct of PIB, a novel synthetic approach was developed for the preparation of PIB-PTX conjugates with pendant carboxylic acids with or without PS arms. The PTX content of these materials was 21 wt% in the absence of PS arms and 10 wt% in the presence of 12 wt% PS arms. The drug release from these materials was found to be slower than that from physical

mixtures of SIBS and PTX, but faster than from previous conjugates, likely due to the polarity of the pendant carboxylic acids. Thermal and AFM analyses suggested that the PTX was quite uniformly distributed in the materials, resulting in homogeneous films that did not undergo significant topographical changes during the 35-day drug release study. The Young's modulus and elongation at break of both **PIB-PTX-COOH** and **PIB-PS-PTX-COOH** were both very similar to those of butyl rubber, whereas the ultimate tensile strength was 10-fold greater than butyl rubber. This may result from the PTX, COOH, or PS moieties, all of which have been shown to increase the tensile strength. Adhesivity of the materials to stainless steel was also investigated and it was found that the incorporation of carboxylic acids and PS increased the adhesion of the coatings. In the drug release study, this translated into the coatings remaining intact and adhered to the stainless steel surface whereas the SIBS control sample tended to degrade and delaminate. An MTT assay demonstrated that none of the evaluated materials released toxic levels of PTX, but the presence of PTX in the films nevertheless inhibited the growth of C2C12 cells on the coatings. Overall, these results provide new insights into the structure-property relationships for PIB-based stent coatings and suggest these materials warrant further study for this application.

Acknowledgements

The authors thank LANXESS and the Natural Sciences and Engineering Research Council of Canada (NSERC) for funding this work, and LANXESS for providing the butyl rubber starting materials. The authors thank Aneta Borecki for assistance with the MTT assay and cellular imaging, Dr. Karen Nygard and the BIOTRON facility for assistance with the cellular imaging and Dr. Heng-Yong Nie of Surface Science Western for assistance with the AFM measurements.

References

1. L. Pinchuk, G. J. Wilson, J. J. Barry, R. T. Schoephoerster, J.-M. Parel, J. P. Kennedy, *Biomaterials* **2008,** *29*, 448-460.
2. J. E. Puskas, L. G. Muñoz-Robledo, R. A. Hoerr, J. Foley, S. P. Schmidt, M. Evancho-Chapman, J. Dong, C. Frethem, G. Haugstad, *Wiley Interdiscip. Rev.: Nanomed. Nanobiotechnol.* **2009,** *1*, 451-462.
3. K. R. Kamath, J. J. Barry, K. M. Miller, *Adv. Drug Delivery Rev.* **2006,** *58*, 412-436.
4. P. B. Schiff, J. Fant, S. B. Horwitz, *Nature* **1979,** *277*, 665-667.
5. M. A. Jordan, L. Wilson, *Nat. Rev. Cancer* **2004,** *4*, 253-265.
6. G. W. Stone, J. W. Moses, S. G. Ellis, J. Schofer, K. D. Dawkins, M.-C. Morice, A. Colombo, E. Schampaert, E. Grube, A. J. Kirtane, D. E. Cutlip, M. Fahy, S. J. Pocock, R. Mehran, M. B. Leon, *N. Engl. J. Med.* **2007,** *356*, 998-1008.
7. A. J. D. Magenau, J. W. Chan, C. E. Hoyle, R. F. Storey, *Polym. Chem.* **2010,** *1*, 831-833.
8. S. Ummadisetty, J. P. Kennedy, *J. Polym. Sci., Part A: Polym. Chem.* **2008,** *46*, 4236-4242.
9. A. J. D. Magenau, T. R. Hartlage, R. F. Storey, *J. Polym. Sci., Part A: Polym. Chem.* **2010,** *48*, 5505-5513.
10. V. Percec, S. Guhaniyogi, J. Kennedy, B. Ivan, *Polym. Bull. (Heidelberg, Ger.)* **1982,** *8*, 25-32.
11. P. Kurian, S. Zschoche, J. P. Kennedy, *J. Polym. Sci., Part A: Polym. Chem.* **2000,** *38*, 3200-3209.
12. B. Gao, J. Kops, *Polym. Bull. (Heidelberg, Ger.)* **1995,** *34*, 279-286.
13. J. M. Rooney, *J. Polym. Sci., Polym. Chem. Ed.* **1981,** *19*, 2119-2122.
14. S. Kéki, M. Nagy, G. Deák, A. Lévai, M. Zsuga, *J. Polym. Sci., Part A: Polym. Chem.* **2002,** *40*, 3974-3986.
15. M. Groenewolt, T. Brezesinski, H. Schlaad, M. Antonietti, P. W. Groh, B. Iván, *Adv. Mater. (Weinheim, Ger.)* **2005,** *17*, 1158-1162.
16. S. Ummadisetty, D. L. Morgan, C. D. Stokes, R. F. Storey, *Macromolecules* **2011,** *44*, 7901-7910.
17. B. Iván, J. P. Kennedy, *J. Polym. Sci., Part A: Polym. Chem.* **1990,** *28*, 89-104.
18. A. Lange, H. Mach, H. P. Rath, K. Ulrich, B. Ivan, P. W. Groh, Z. T. Nagy, V. Palfi WO Patent 2004101631, Nov 25, 2004.
19. P. Viktoria, B. Iván, *PMSE Prepr.* **2009,** *101*, 874-876.
20. R. F. Storey, A. D. Scheuer, B. C. Achord, *Polymer* **2005,** *46*, 2141-2152.
21. F. P. Baldwin, *Rubber Chem. Technol.* **1979,** *52*, 77-84.
22. G. E. Jones, D. S. Tracey, A. L. Tisler, Halogenated Butyl Rubber. In Rubber Technolology, Compounding and Testing for Performance, Dick, J. S., Ed. Hanser: Munich, 2001; pp 178-189.
23. S. M. Malmberg, J. S. Parent, D. A. Pratt, R. A. Whitney, *Macromolecules* **2010,** *43*, 8456-8461.
24. J. S. Parent, A. Penciu, S. A. Guillén-Castellanos, A. Liskova, R. A. Whitney, *Macromolecules* **2004,** *37*, 7477-7483.
25. J. S. Parent, D. J. Thom, G. White, R. A. Whitney, W. Hopkins, *J. Polym. Sci., Part A: Polym. Chem.* **2001,** *39*, 2019-2026.

26. J. S. Parent, G. D. F. White, R. A. Whitney, *J. Polym. Sci., Part A: Polym. Chem.* **2002,** *40*, 2937-2944.
27. S. Xiao, J. S. Parent, R. A. Whitney, L. K. Knight, *J. Polym. Sci., Part A: Polym. Chem.* **2010,** *48*, 4691-4696.
28. S. Yamashita, K. Kodama, Y. Ikeda, S. Kohjiya, *J. Polym. Sci., Part A: Polym. Chem.* **1993,** *31*, 2437-2444.
29. J. K. McLean, S. A. Guillen-Castellanos, J. S. Parent, R. A. Whitney, R. Resendes, *Eur. Polym. J.* **2007,** *43*, 4619-4627.
30. J. K. McLean, S. A. Guillén-Castellanos, J. S. Parent, R. A. Whitney, K. Kulbaba, A. Osman, *Ind. Eng. Chem. Res.* **2009,** *48*, 10759-10764.
31. C. V. Bonduelle, E. R. Gillies, *Macromolecules* **2010,** *43*, 9230-9233.
32. C. V. Bonduelle, S. Karamdoust, E. R. Gillies, *Macromolecules* **2011,** *44*, 6405-6415.
33. S. Karamdoust, C. V. Bonduelle, R. C. Amos, B. A. Turowec, S. Guo, L. Ferrari, E. R. Gillies, *J. Polym. Sci., Part A: Polym. Chem.* **2013,** *51*, 3383-3394.
34. M. J. McEachran, J. F. Trant, I. Sran, J. R. de Bruyn, E. R. Gillies, *Ind. Eng. Chem. Res.* **2015,** *54*, 4763-4772.
35. P. Antony, S. K. De, *J. Macromol. Sci., Part C: Polym. Rev.* **2001,** *41*, 41-77.
36. A. Ozvald, J. Scott Parent, R. A. Whitney, *J. Polym. Sci., Part A: Polym. Chem.* **2013,** *51*, 2438-2444.
37. A. Zosel, *Adv. Pressure Sensitive Adhes. Technol.-1* **1992,** *1*, 92-127.
38. R. Vendamme, K. Olaerts, M. Gomes, M. Degens, T. Shigematsu, W. Eevers, *Biomacromolecules* **2012,** *13*, 1933-1944.
39. A. Bellamine, E. Degrandi, M. Gerst, R. Stark, C. Beyers, C. Creton, *Macromol. Mater. Eng.* **2011,** *296*, 31-41.
40. M. M. Abd Rabo Moustafa, E. R. Gillies, *Macromolecules* **2013,** *46*, 6024-6030.
41. J. Iqbal, J. Gunn, P. W. Serruys, *Brit. Med. Bull.* **2013,** *106*, 193-211.
42. T. Hu, J. Yang, K. Cui, Q. Rao, T. Yin, L. Tan, Y. Zhang, Z. Li, G. Wang, *ACS Appl. Mater. Interfaces* **2015,** *7*, 11695-11712.
43. S. Garg, P. W. Serruys, *J. Am. Coll. Cardiol.* **2010,** *56*, S1-S42.
44. P. A. Lemos, P. W. Serruys, R. T. van Domburg, F. Saia, C. A. Arampatzis, A. Hoye, M. Degertekin, K. Tanabe, J. Daemen, T. K. K. Liu, E. McFadden, G. Sianos, S. H. Hofma, P. C. Smits, W. J. van der Giessen, P. J. de Feyter, *Circulation* **2004,** *109*, 190-195.
45. P. W. Serruys, M. J. B. Kutryk, A. T. L. Ong, *N. Engl. J. Med.* **2006,** *354*, 483-495.
46. S. K. James, U. Stenestrand, J. Lindbäck, J. Carlsson, F. Scherstén, T. Nilsson, L. Wallentin, B. Lagerqvist, *N. Engl. J. Med.* **2009,** *360*, 1933-1945.
47. T. Inoue, K. Node, *Circ. J.* **2009,** *73*, 615-621.
48. Y. Levy, D. Mandler, J. Weinberger, A. J. Domb, *J. Biomed. Mater. Res., Part B* **2009,** *91B*, 441-451.
49. J. A. Ormiston, E. Currie, M. W. I. Webster, P. Kay, P. N. Ruygrok, J. T. Stewart, R. C. Padgett, M. J. Panther, *Catheter. Cardio. Inte.* **2004,** *63*, 332-336.
50. K. Ren, M. Zhang, J. He, Y. Wu, P. Ni, *ACS Appl. Mater. Interfaces* **2015,** *7*, 11263-11271.
51. P. A. Hårdhammar, H. M. M. van Beusekom, H. U. Emanuelsson, S. H. Hofma, P. A. Albertsson, P. D. Verdouw, E. Boersma, P. W. Serruys, W. J. van der Giessen, *Circulation* **1996,** *93*, 423-430.

52. M. C. M. Vrolix, V. M. Legrand, J. H. C. Reiber, G. Grollier, M. J. Schalij, P. Brunel, L. Martinez-Elbal, M. Gomez-Recio, F. W. H. M. Bär, M. E. Bertrand, A. Colombo, J. Brachman, *Am. J. Cardiol.* **2000,** *86*, 385-389.
53. J. Zhao, R. Falotico, T. Nguyen, Y. Cheng, T. Parker, V. Davé, C. Rogers, J. Riesenfeld, *J. Biomed. Mater. Res., Part B* **2012,** *100B*, 1274-1282.
54. M.-C. Chen, Y. Chang, C.-T. Liu, W.-Y. Lai, S.-F. Peng, Y.-W. Hung, H.-W. Tsai, H.-W. Sung, *Biomaterials* **2009,** *30*, 79-88.
55. J. Ako, H. N. Bonneau, Y. Honda, P. J. Fitzgerald, *Am. J. Cardiol.* **2007,** *100*, S3-S9.
56. J. Li, D. Li, F. Gong, S. Jiang, H. Yu, Y. An, *BioMed Res. Int.* **2014,** *2014*, Article ID 902782.
57. J. F. Trant, M. McEachran, I. Sran, B. A. Turowec, J. R. de Bruyn, E. R. Gillies, *ACS Appl. Mater. Interfaces* **2015,** *7*, 14506-14517.
58. J. F. Trant, I. Sran, J. R. De Bruyn, M. Ingratta, A. Borecki, E. R. Gillies, *Eur. Polym. J.* **2015,** *72*, 148-162.
59. S. Karamdoust, P. Crewdson, M. Ingratta, E. R. Gillies, *Polym. Int.* **2015,** *64*, 611-620.
60. ASTM, Standard Test Method for Tensile Properties of Thin Plastic Sheeting. ASTM: New York, 2012; Vol. D882-12.
61. H. M. Deutsch, J. A. Glinski, M. Hernandez, R. D. Haugwitz, V. L. Narayanan, M. Suffness, L. H. Zalkow, *J. Med. Chem.* **1989,** *32*, 788-792.
62. H. Lataste, V. Senilh, M. Wright, D. Guénard, P. Potier, *Proc. Natl. Acad. Sci. U.S.A.* **1984,** *81*, 4090-4094.
63. I. Franta, Editor, Studies in Polymer Science, 1: Elastomers and Rubber Compounding Materials. Elsevier: New York, 1989; p 607.
64. N. Willenbacher, O. Lebedeva, Polyisobutylene-based pressure-sensitive adhesives. In Handbook of pressure sensitive adhesives and products, Benedek, I.; Feldstein, M. M., Eds. Taylor and Francis Group: Boca Raton, La, 2009; pp 4.1-4.18.
65. G. Erdödi, B. Iván, *Chem. Mater.* **2004,** *16*, 959-962.
66. Y. Ikeda, K. Kodama, K. Kajiwara, S. Kohjiya, *J. Polym. Sci., Part B: Polym. Phys.* **1995,** *33*, 387-394.
67. A. L. Gergely, J. E. Puskas, *J. Polym. Sci., Part A: Polym. Chem.* **2015,** *53*, 1567-1574.
68. J. H. Roh, D. Roy, W. K. Lee, A. L. Gergely, J. E. Puskas, C. M. Roland, *Polymer* **2015,** *56*, 280-283.
69. J. E. Puskas, A. L. Gergely, G. Kaszas, *J. Polym. Sci., Part A: Polym. Chem.* **2013,** *51*, 29-33.
70. L. Sipos, A. Som, R. Faust, R. Richard, M. Schwarz, S. Ranade, M. Boden, K. Chan, *Biomacromolecules* **2005,** *6*, 2570-2582.
71. F. Strickler, R. Richard, S. McFadden, J. Lindquist, M. C. Schwarz, R. Faust, G. J. Wilson, M. Boden, *J. Biomed. Mater. Res., Part A* **2010,** *92A*, 773-782.
72. R. W. Sirianni, E.-H. Jang, K. M. Miller, W. M. Saltzman, *J. Controlled Release* **2010,** *142*, 474-482.
73. J. Joshi, R. Lehman, T. Nosker, *J. Appl. Polym. Sci.* **2006,** *99*, 2044-2051.
74. P. Antony, J. E. Puskas, M. Kontopoulou, *Polym. Eng. Sci.* **2003,** *43*, 243-253.
75. C. L. Rao, J. J. Connor, *J. Adhes.* **1993,** *43*, 179-197.
76. R. Resendes, R. Krista, J. N. Hickey U.S. Patent 7,662,480, Feb 22, 2007.
77. F. H. Strickler U. S. Patent 8,092,821 B2, Jan 10, 2012.

78. D. T. Vistica, P. Skehan, D. Scudiero, A. Monks, A. Pittman, M. R. Boyd, *Cancer Res.* **1991,** *51*, 2515-2520.
79. Tests for *in vitro* Cytotoxicity. In *Biological Evaluation of Medical Devices*, ISO: Geneva, Switzerland, 2009; Vol. 10993-5.